RSC Advances

PAPER

View Article Online
View Journal | View Issue

Cite this: *RSC Adv.*, 2021, **11**, 29948

A novel superparamagnetic powerful guanidine-functionalized γ-Fe_2O_3 based sulfonic acid recyclable and efficient heterogeneous catalyst for microwave-assisted rapid synthesis of quinazolin-4(3*H*)-one derivatives in Green media†

Fateme Haji Norouzi,[a] Naser Foroughifar, *[a] Alireza Khajeh-Amiri[b] and Hoda Pasdar[a]

The novel organic–inorganic nanohybrid superparamagnetic (γ-Fe_2O_3@CPTMS–guanidine@SO_3H) nanocatalyst modified with sulfonic acid represents an efficient and green catalyst for the one-pot synthesis of quinazolin-4(3*H*)-one derivatives *via* three-component condensation reaction between anthranilic acid, acetic anhydride and different amines under microwave irradiation and solvent-free conditions (**4a–q**). XRD, FT-IR, FE-SEM, TGA, VSM and EDX were used to characterize this new magnetic organocatalyst. Outstanding performance, short response time (15–30 min), simple operation, easy work-up procedure, and avoidance of toxic catalysts can be regarded as its significant advantages. Moreover, it can be easily separated from the reaction solution through magnetic decantation using an external magnet, and recycled at least six times without notable reduction in its activity.

Received 20th July 2021
Accepted 26th August 2021

DOI: 10.1039/d1ra05560g

rsc.li/rsc-advances

1 Introduction

In recent years, green nano-synthesis has become a significant challenge in synthetic organic chemistry, applying effective and eco-friendly procedures in synthesizing biological products.[1,2] As a heterogeneous catalyst, applying this nanomaterial has become popular in organic synthesis because of its surface modification ability, ease of synthesis and separation, excellent surface area, environmentally benign nature, high thermal and chemical stability, simple and efficient workup method, low cost, and reusability,[3–5] Magnetic nanoparticles (MNPs) have been recognized as environmentally benign alternatives to conventional base catalysts and Lewis acids in various processes.[6] Hence, non-toxic catalyzed organic MNP processes such as with maghemite (γ-Fe_2O_3) and magnetite (Fe_3O_4) typically consume a minimum of energy and reagents or auxiliaries in order to follow the principles of green chemistry and minimize waste.[7–9]

Surface sulfonation of MNPs with chlorosulfonic acid (HSO_3Cl) is an appropriate, acceptable, fast, effective and easy method to produce acidic heterogeneous magnetic nanocatalysts with higher catalytic efficiency.[9,10] In this sense, the first step was to describe a green synthesis path in order to prepare an efficient, leak-free and reusable multi-functional heterogeneous magnetic nanocatalyst *via* linking the SO_3H groups onto MNPs' surface coated with guanidine as an efficacious bridge. As a bridge with three functional heads, it can be regarded as a COOH moiety with a solid affinity for γ-Fe_2O_3@CPTMS surface hydroxyl groups and NH groups for the grafting of multi-SO_3H functionalities (Scheme 1).

However, regarding the low-cost and environment friendly criteria, multi-component reactions (MCRs), combining more than two components in a single synthetic operation, have gained ecological importance – aiming at synthesizing the highly significant chemical and biological organic frameworks. It is worth mentioning that when these processes are applied, we will have the following advantages: the isolation and purification of intermediates are avoided, higher productivity will be reached, solvent waste will be minimized, and transformations' greenness will also be enhanced.[11,12]

Moreover, MW-assisted organic synthesis (MAOS) has become a valuable tool, improving the result of MCRs[13] due to microwave heating. Besides, it can minimize side reactions, reduce reaction times, increase yields, improve reproducibility, and – even with ordinary heating – make the inaccessible reactions possible. Furthermore, MW-assisted organic

[a]*Department of Chemistry, Tehran North Branch, Islamic Azad University, Tehran, Iran. E-mail: n_foroughifar@yahoo.com*

[b]*Toxicology Research Center, Aja University of Medical Sciences, Tehran, Iran*

† Electronic supplementary information (ESI) available. See DOI: 10.1039/d1ra05560g

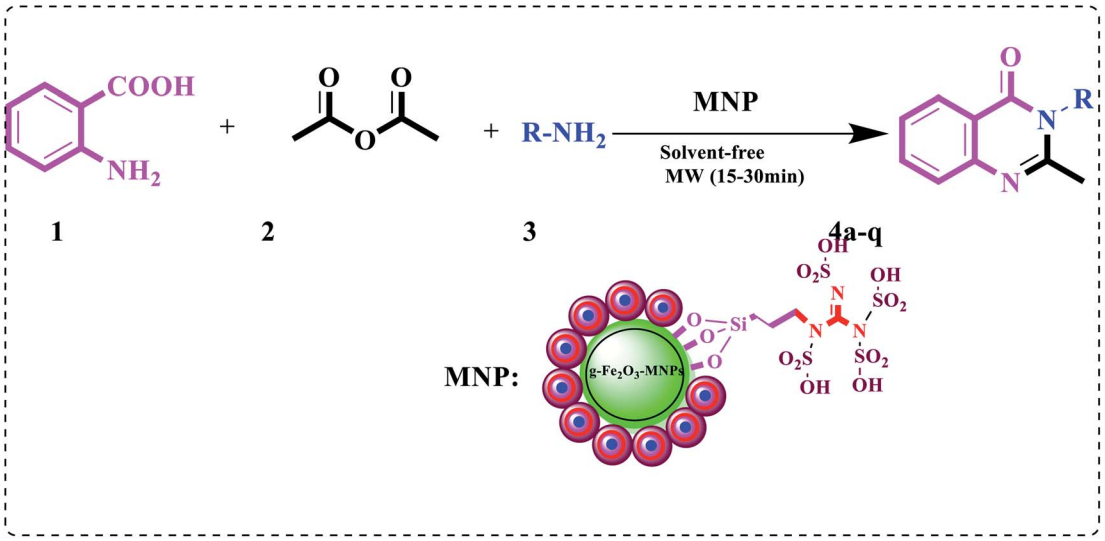

Scheme 1 One-pot, three-component synthesis of quinazolin-4(3*H*)-one derivatives in the presence of γ-Fe_2O_3@CPTMS–guanidine@SO_3H as catalyst.

synthesis (MAOS) is particularly useful in preparing diverse biologically active heterocyclic compounds.[14]

Regarding the organic and medicinal chemistry, N-heterocycles have been regarded as the most essential building blocks. Accordingly, considering medicinal chemistry, quinazolinone derivatives have received great attention due to their broad spectrum of biological activities, *i.e.* antibacterial,[15] anti-inflammatory,[16] antifungal,[17] anticancer,[18] antimalarial,[19] anti-aggregating,[20] anticonvulsant,[21] antidepressant,[20] antihistaminic,[18] anti-hypoglycemic,[19] antimalarial,[22] anti-obesities,[23] insecticidal[24] antidepressants, and neurological activities.

It is worth mentioning that quinazolin-4(3*H*)-one, which can be regarded as a heterocyclic nucleus, can be broadly found in different bioactive natural products of medicinal plants, *i.e.* febrifugine,[25] vasicinone,[26] luotonin A,[26] tryptanthrin[27] (Fig. 1), and so on.[24] Natural quinazolin-4(3*H*)-ones can have important applications, pointing to future developments as bioactive lead compounds.[15]

Although different synthetic methods have been introduced for the preparation of quinazolinone derivatives, a wide variety of these procedures has been reported in the presence of different types of catalysts, *i.e.* the replacement of pollutive inorganic acid catalysts – such as H_2SO_4 or HCl – with reusable solid acids seems still very necessary. In this sense, heterogenization of the existing homogeneous catalysts – using solid support material *via* chemical anchoring of the reactive centers of the traditional organic acid onto an inorganic solid supports – rendered an excellent strategy for the production and design of the superior heterogeneous hybrid catalysts. Furthermore, such catalysts would result in exhibiting better performance, selectivity and stability and

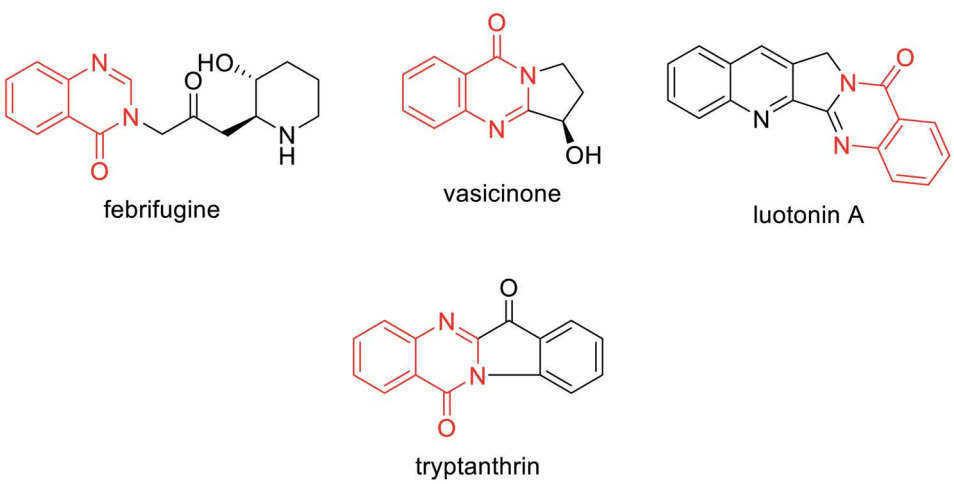

Fig. 1 Some quinazolin-based drugs and drug-like candidates.

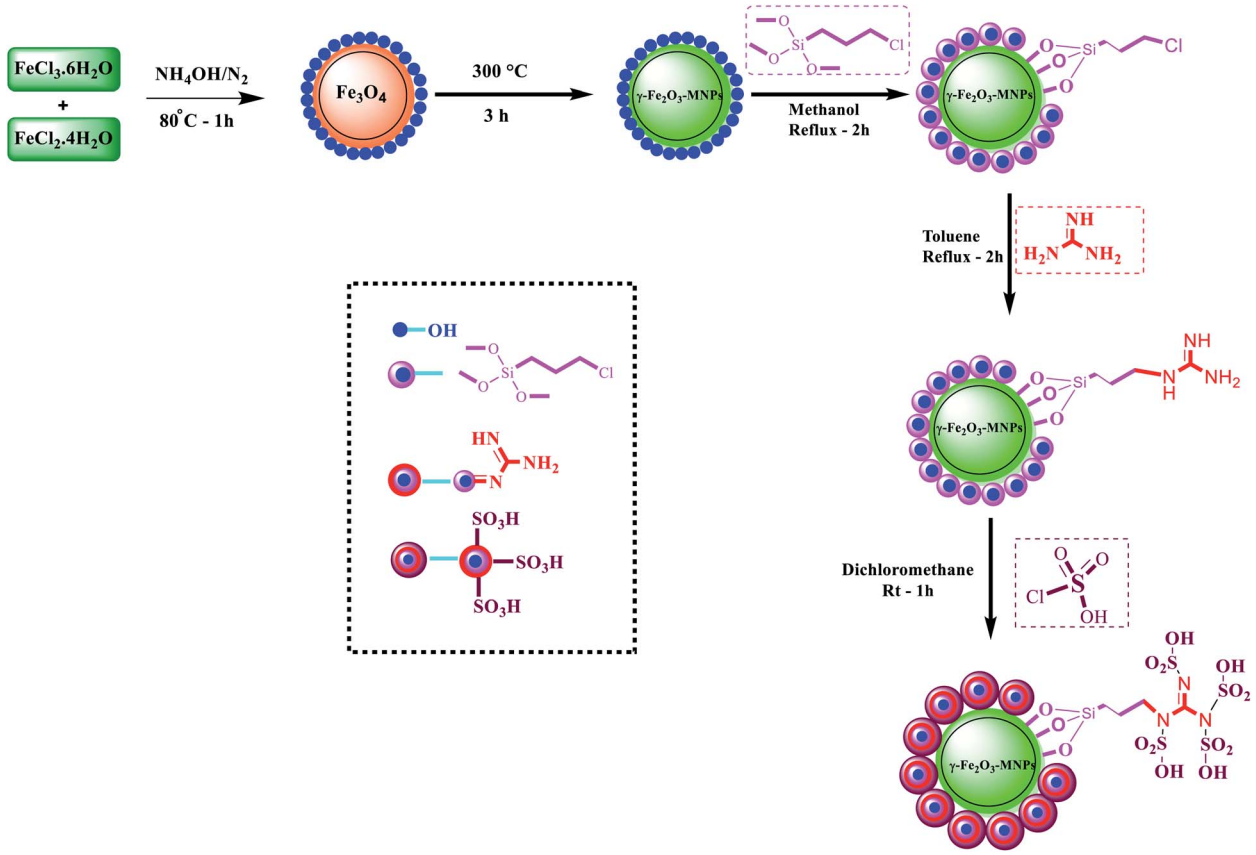

Scheme 2 Synthesis of γ-Fe_2O_3@CPTMS–guanidine@SO_3H as new heterogeneous catalyst.

also permitting catalyst recovery, as the basic feature of green chemistry.

Accordingly, regarding our previous study on multi-component reactions and our ongoing project to synthesize complex organic compounds; herein, we aim at,[11] applying nano and green chemistry to design an efficient, heterogeneous and reusable catalyst. Moreover, we also try to investigate the utility of the newly synthesized metal–organic framework γ-Fe_2O_3@CPTMS–guanidine@SO_3H as a core–shell structured nanocatalyst for the synthesis of a series of quinazolin-4(3*H*)-one derivatives (**4a–q**) under microwave irradiation (180 W, max. 70 °C) in solvent-free condition (Scheme 1).

2. Results and discussion

Herein, a new core–shell nanomagnetic silica, as it is coated with guanidine spacer and sulfonic acid tag, is reported for the synthesis of quinazolin-4(3*H*)-one derivatives. At first, we

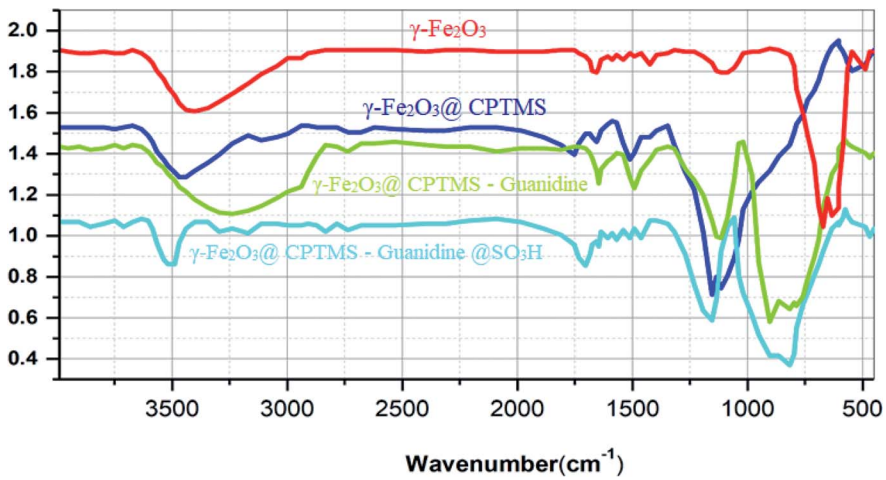

Fig. 2 FT-IR spectra: γ-Fe_2O_3@CPTMS–guanidine@SO_3H.

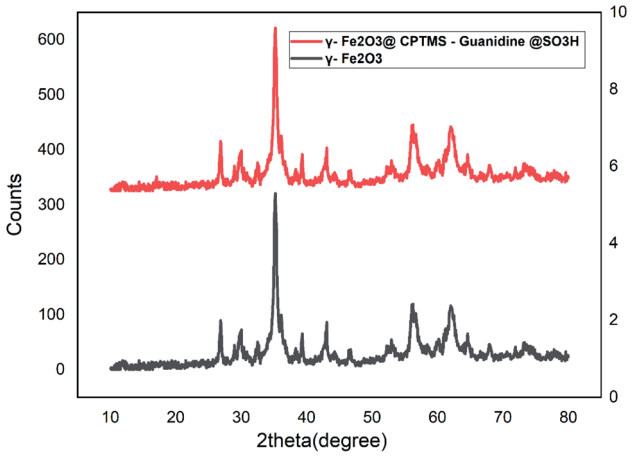

Fig. 3 XRD spectra of γ-Fe_2O_3@CPTMS–guanidine@SO_3H.

aimed at synthesizing the superparamagnetic Fe_3O_4 nanoparticles, applying the chemical co-precipitation method from ferrous and ferric ions in ammonia solution having minor modifications.[28–30] Subsequently, we witnessed the conversion of, the nanoparticles to γ-Fe_2O_3 at 300 °C for 3 h. Besides, in order to have the chloropropyl-functionalized magnetic nanoparticles, γ-Fe_2O_3 was coated with 3-chloropropyltrimethoxysilane (CPTMS). It is worth mentioning that when chloropropyl group reacted with guanidine, the result was the corresponding guanidine supported on the magnetic nanoparticles. Ultimately, the reaction of sulfonic acid with guanidine formed new superparamagnetic silica-encapsulated γ-Fe_2O_3 as the catalyst (Scheme 2). γ-Fe_2O_3@CPTMS–guanidine@SO_3H as a novel, green and task-specific catalyst was characterized using different techniques and, then, its potential as a catalyst was analyzed. Significantly, we aimed at characterizing the magnetic nanocatalyst structure applying different techniques, *i.e.* X-ray diffraction (XRD), Fourier transform infrared (FT-IR) spectroscopy, transmission electron microscopy (TEM), scanning electron microscopy (SEM), thermogravimetric analysis (TGA), vibrating sample magnetometry (VSM), energy-dispersive X-ray spectroscopy (EDS), Brunauer–Emmett–Teller (BET) and Raman spectroscopy.

Fig. 2 illustrates the FT-IR spectrum of γ-Fe_2O_3@CPTMS–guanidine@SO_3H. Herein, we can observe the following stretching vibrations: Fe–O near 581 cm^{-1}, O–H at 3300–3500 cm^{-1}, Si–O at 1000–1110 cm^{-1}, C–O at 1600–1752 cm^{-1} and C–H at 2945 cm^{-1}. Accordingly, the sulfonic acid's successful attachment on the surface of γ-Fe_2O_3@CPTMS nanoparticles can be proved.

Fig. 3 illustrates the XRD of the bare MNPs, clarifying the fact that the pattern is consistent with those of the described spinel ferrites. The intensities and positions of all peaks accord with the standard XRD pattern of Fe_2O_3 MNPs (JCPDS card no. 85-1436), showing the retention of the crystalline cubic spinel structure of MNPs. In this regard, nine characteristic peaks are revealed, as clearly indicated in Fig. 3:

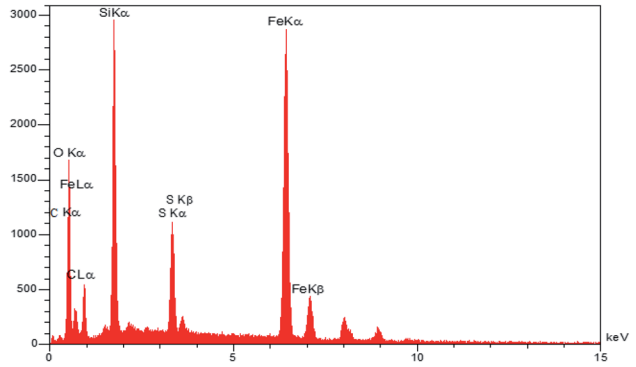

Fig. 4 EDAX spectra of γ-Fe_2O_3@CPTMS–guanidine@SO_3H.

EDS result (Fig. 4) shows Fe, O, Si, C, N, and S signals, indicating the functionalized iron oxide nanoparticles and confirming the successful synthesis of γ-Fe_2O_3@CPTMS–guanidine@SO_3H MNPs.

Thermal gravimetric analysis was applied to appraise the stability of the γ-Fe_2O_3@CPTMS–guanidine@SO_3H and bond formation between Fe_3O_4 and organic agent. As evident in Fig. 5, the TGA curve would reveal that the first weight loss below 100 °C would be associated to the solvent desorption and surface hydroxyl groups. The second weight loss can be related to the sulfonic acid decomposition, as grafted on the γ-Fe_2O_3 MNPs surface. It is worth mentioning that the TGA curve reveals the value of sulfonic acid to be about 6.6%.

To evaluate the magnetic properties of γ-Fe_2O_3@CPTMS–guanidine@SO_3H (Fig. 6), the saturation magnetization (MS) quantities for γ-Fe_2O_3 and γ-Fe_2O_3@CPTMS–guanidine@SO_3H catalyst are approximately 57 emu g^{-1} and 45 emu g^{-1}, respectively. The MS of γ-Fe_2O_3@CPTMS–guanidine@SO_3 catalyst, as compared to the uncoated γ-Fe_2O_3 MNPs (57.22 emu g^{-1}), showed a great deal of decrease due to the fact that

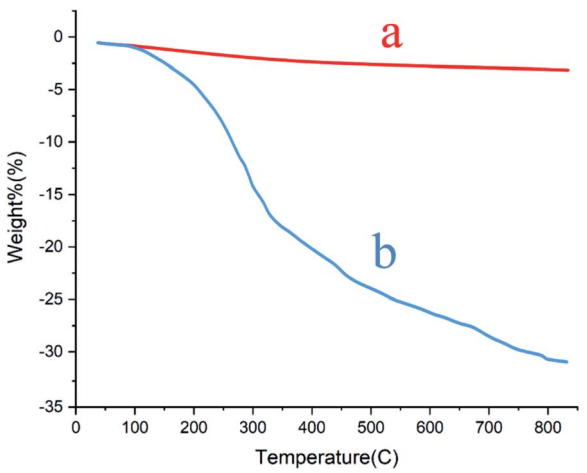

Fig. 5 TGA patterns of (a) γ-Fe_2O_3 and (b) the γ-Fe_2O_3@CPTMS–guanidine@SO_3H MNRs.

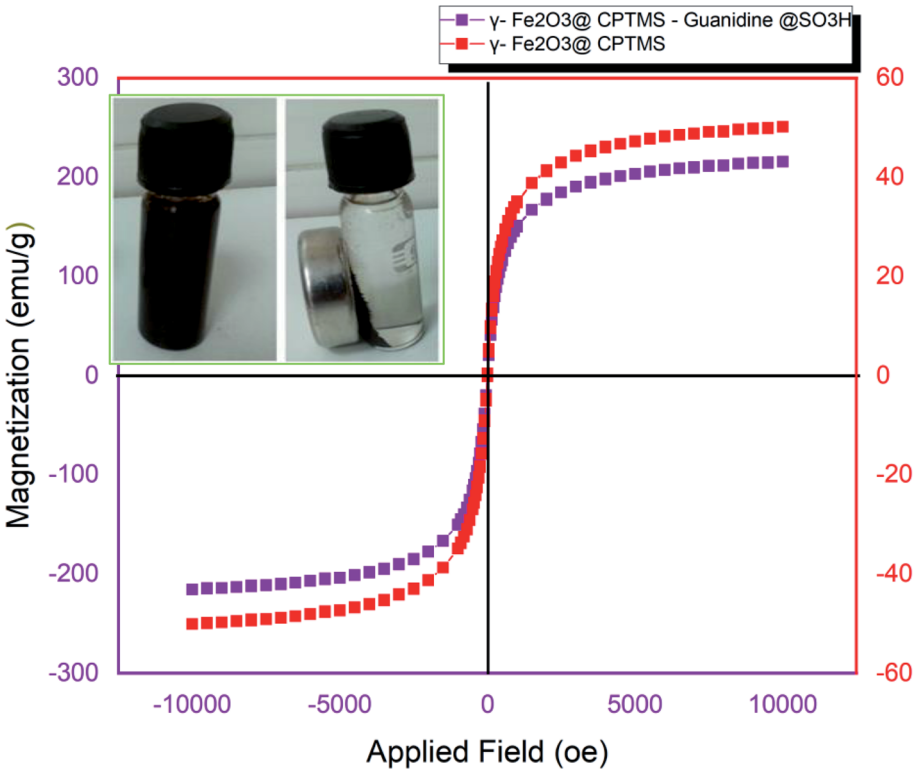

Fig. 6 VSM diagrams of γ-Fe_2O_3@CPTMS–guanidine@SO_3H and γ-Fe_2O_3, the picture displays the catalyst was dispersed in liquid and captured by the outer magnet.

the organic compound on the nanoparticles surface was increased. Furthermore, as seen in Fig. 6 (right inset), we aimed at specifying the strong magnetization of the MNPs using an external magnet.

In order to distinguish the iron oxides phases, Raman spectroscopy would be applied. Moreover, we applied a confocal Raman microscope collecting the spectra of the nanocatalysts (Fig. 7) at several regions of each sample. In this sense, the spectra illustrate the main band at 666 cm^{-1}, assigned to the symmetric stretch of oxygen atoms along Fe–O bonds (A_{1g}) of magnetite. Besides, the bands at 500 (T_{2g}), 717 (A_{1g}), and 357 (E_g) cm^{-1} can be related to maghemite. Accordingly, it is worth mentioning that the prepared catalysts would be made from the magnetite and maghemite phases of iron oxide.

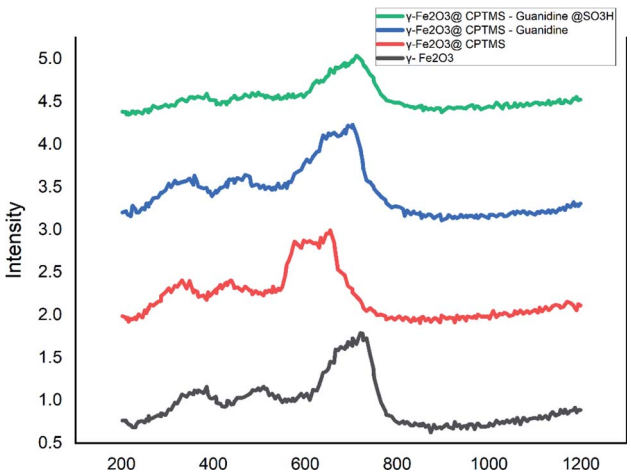

Fig. 7 Raman spectra of the γ-Fe_2O_3@CPTMS–guanidine@SO_3H the magnetic nanocatalysts.

The applied SEM analysis aimed at assaying the surface morphology of the obtained nanocatalysts (Fig. 8). The SEM images illustrate the homogeneous size and shape of the particles with an average size of 35 nm.

In order to evaluate the particle size and morphology of the synthesized γ-Fe_2O_3@CPTMS–guanidine@SO_3H acid MNPs, transmission electron microscopy was performed (Fig. 9) which indicates the uniform-sized particles with an average size of 50 nm.

BET can be considered as an important method for measuring the specific surface area of materials (SSA). The following formula can be applied in order to calculate the average particle diameter (nm): $d_{BET} = 6000/\tilde{n}s$.

In this formula, s can be regarded as the specific surface area in $m^2\ g^{-1}$ and $\tilde{n}$ is the theoretical density in g cm^{-1}.[3,28,29] Regarding the surface area measurement, when solid particles are not united, we have the nitrogen gas (N_2) accessing the holes and the powder surface. Finally, a good measurement of the actual particle size obtained from the density is witnessed. Herein, the obtained specific surface area was at about

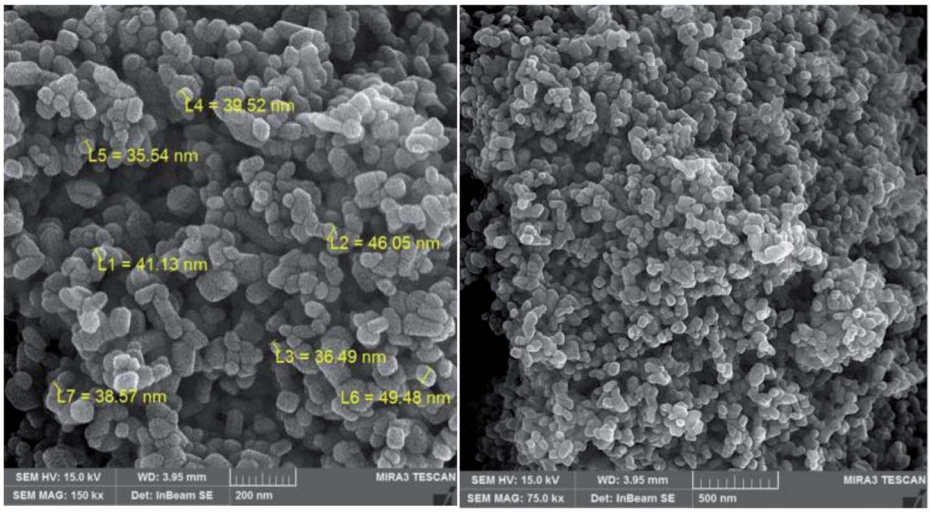

Fig. 8 SEM image of γ-Fe_2O_3@CPTMS–guanidine@SO_3H.

60.5 $m^2\ g^{-1}$ and the calculated mean particle size (27 nm) was close to the TEM value (Fig. 10).

2.1. Synthesis of quinazolin-4(3*H*)-one

Regarding the significance of quinazoline derivatives, we aimed at finding a practical method in order to synthesize them with high yields and purity. In this regard, developing efficient and environment friendly procedures has always been desirable. Accordingly, we tried to peruse whether those quinazolin-4(3*H*)-one derivatives can be prepared by condensation of anthranilic acid, acetic anhydride and different amines in solvent-free condition under microwave irradiation, which would result in increasing the yields, reducing the amount of waste material and shortening the reaction period. In this sense, the condensation reaction was selected as the model reaction as it was between anthranilic acid, **1** (1 mmol), acetic anhydride **2** (1 mmol) and ammonium acetate **3**, in order to synthesize compound **4a** in the presence of various catalytic systems under microwave irradiation in solvent-free condition (Scheme 3). Besides, Table 1 shows the obtained the results. Furthermore, when screening was performed, it was revealed that the optimized yields and time profiles were reached when the reaction was performed in the presence of 0.05 g of γ-Fe_2O_3@CPTMS–guanidine@SO_3H in solvent-free condition and under microwave irradiation, leading to 2-methylquinazolin-4(3*H*)-one **4a** in 15 min with 92% of yield (Table 1, entry 8). Notably, when the amount of γ-Fe_2O_3@CPTMS–guanidine@SO_3H was increased to 0.08 g, we witnessed no yield improvement; whereas, when we decreased the amount of the catalyst to 0.015 g, the yield also decreased. Besides, an efficient progress in the reaction was not witnessed in the absence of γ-Fe_2O_3@CPTMS–guanidine@SO_3H even after 35 minutes under microwave irradiation.

Herein, no solvent was analyzed due to the green chemistry concept. Regarding the scope of the reaction, we aimed at extending our study to different amines applying the optimized conditions. As seen in Table 2, an efficient progress of the reaction is indicated, resulted in higher yields without the formation of any side products. According to the same table, an efficient development of the reactions was witnessed applying amines with electron-withdrawing groups rather than substitutions of electron-rich groups on the benzene ring. Moreover, we characterized the pure products, comparing their physical data (melting points, IR and ^{1}H NMR) with those mentioned in the literature. The structural assignments were performed on the basis of IR, ^{1}H NMR, ^{13}C NMR and elemental analysis. The mass spectra showed molecular ion peaks at the appropriate *m*/*z* values.

Catalyst recovery and reuse can be regarded as the greatest advantages in green chemistry and heterogeneous catalysis. It is also industrially important in commercial use and large-scale operations. Accordingly, the recycling of the γ-Fe_2O_3@CPTMS–guanidine@SO_3H was also investigated in solvent-free condition and under microwave irradiation (180 W, max. 70 °C), applying the model reaction of anthranilic acid, acetic anhydride and amines in the presence of Fe_2O_3@CPTMS–guanidine@SO_3H (Table 2, entry 1). When the reaction was completed, hot ethanol was used to dilute the reaction mixture. Furthermore, an external magnetic field was applied to separate the catalyst from the reaction mixture. Subsequently, it was washed with hot ethanol, dried in air and, finally, reused for a similar reaction. Significantly, we reused the recovered homogeneous catalyst six consecutive cycles without any significant decrease in its catalytic performance (Fig. 11).

In order to evaluate the efficiency and generality of this methodology, we aimed at comparing the results obtained from the reaction of anthranilic acid, acetic anhydride and amines with previous procedures (Table 3). Accordingly, the present procedure was found to be significantly superior to the reported procedures.

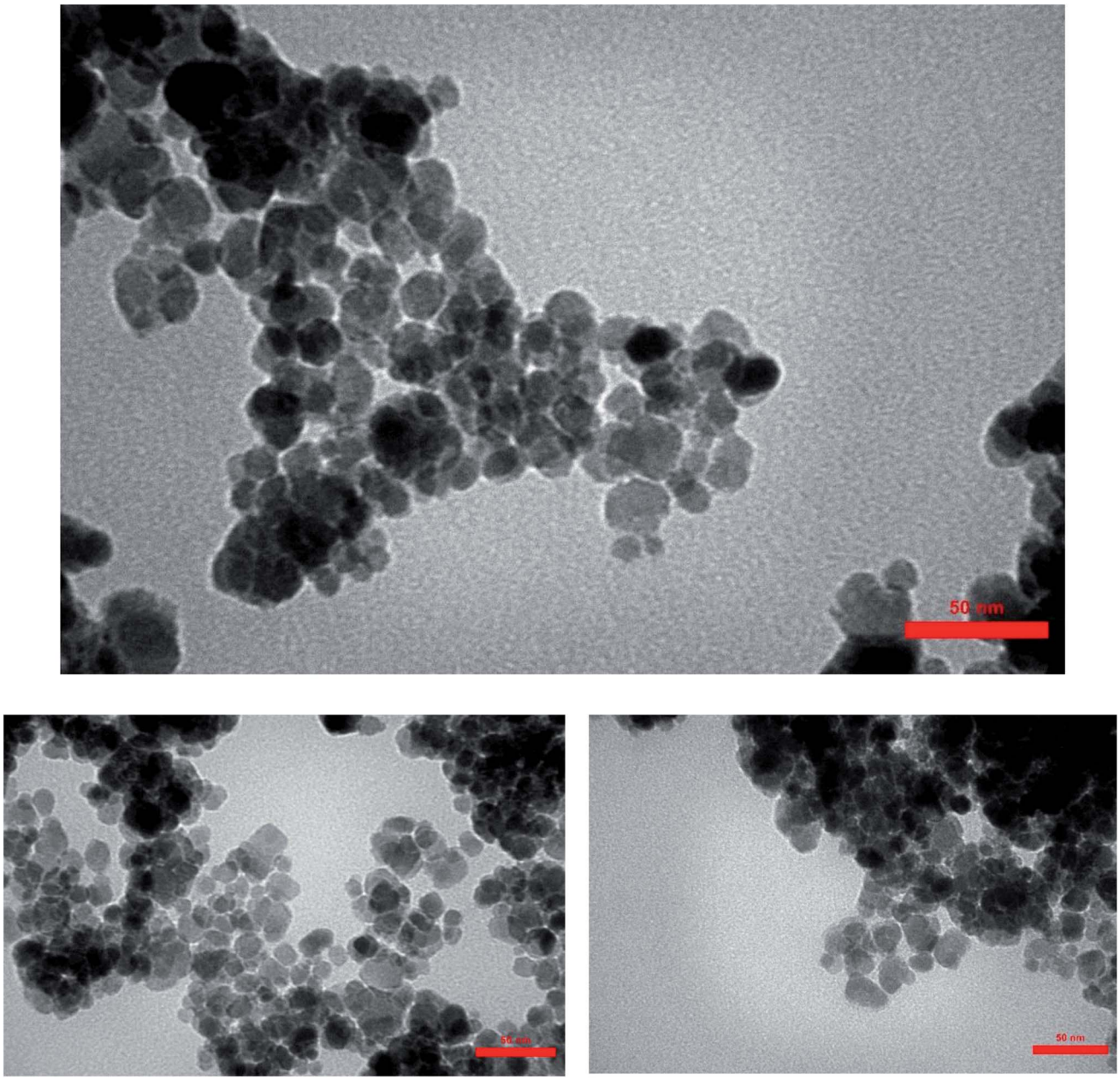

Fig. 9 TEM image of γ-Fe_2O_3@CPTMS–guanidine@SO_3H.

When the catalyst was recycled for about six runs and in order to demonstrate the catalyst stability under microwave irradiation condition and confirm the catalyst recoverability, we analyzed the spent γ-Fe_2O_3@CPTMS–guanidine@SO_3H catalyst using FT-IR, SEM, EDX, XRD, VSM, and TGA techniques (Fig. 12). Interestingly, the results show good agreement with the new catalyst analysis.

3. Conclusions

In summary, we aimed at synthesizing organic–inorganic nanohybrid superparamagnetic nanoparticles of the modified sulfonic acid (γ-Fe_2O_3@SiO_2–guanidine@SO_3H) as an efficient, new, homogeneous, and reusable catalyst. Besides, the catalyst was characterized applying BET, EDS, SEM, XRD, VSM, TGA, FT-IR spectroscopy, and Raman. Notably, we used this novel catalyst as a green heterogeneous organic acid for the efficient synthesis of the functionalized quinazolin-4(3*H*)-one derivatives. The environment friendly methodology possesses significant green chemistry characteristics, *i.e.* using a reusable, easy-to-handle low-loading, and non-toxic catalyst, having shorter reaction time, avoiding hazardous organic solvents, and easy work-up. Furthermore, this attractive atom-economical protocol is expected to produce compounds exhibiting interesting pharmacological activities and may act as potential drug candidates.

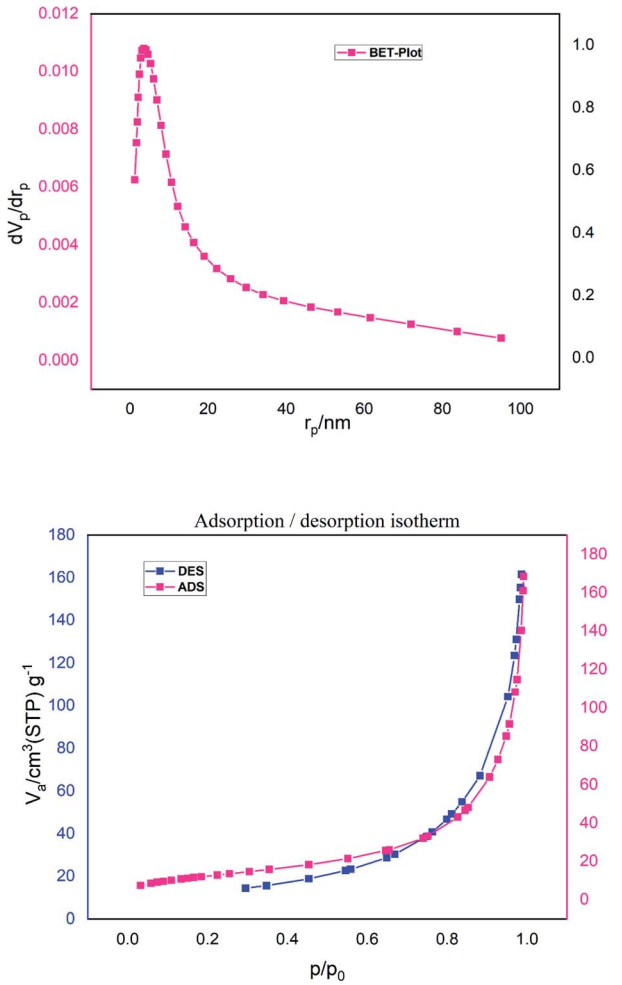

Fig. 10 Nitrogen adsorption–desorption isotherm and the pore size distribution curve (inset) for γ-Fe_2O_3@CPTMS–guanidine@SO_3H.

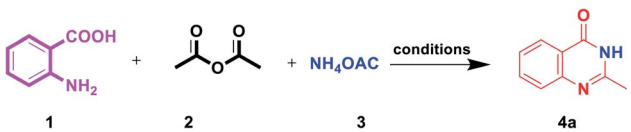

Scheme 3 Synthesis of 2-methylquinazolin-4(3*H*)-one (**4a**).

4. Experimental section

4.1. General

All starting materials and chemicals used in this research were bought from Sigma-Aldrich chemical companies without further purification. All recorded melting points (mp) were taken in an open capillary tube on a Stuart scientific melting-point apparatus and are uncorrected. Elemental analysis was performed on a PerkinElmer 2400 C, H, N analyzer and values were within the acceptable limits of the calculated values. Infrared (FT-IR) spectra of all samples in our study were recorded in the sub-region 400–4000 cm^{-1} on PerkinElmer Spectrum one instruments, using potassium bromide discs. Mass spectra were obtained on a HP 5975 Mass Selective Detector at 70 eV. The proton magnetic resonance ^1H and ^{13}C spectra were performed on Bruker 400 or 600 spectrometers using $CDCl_3$ and DMSO-d_6 as solvent; all with tetramethylsilane (TMS) as internal standard. The chemical shifts were reported in δ value as parts per million (δ ppm) and coupling constants (J) are expressed in hertz (Hz). The following abbreviations were used to explain the multiplicities: br, broad; s, singlet; d, doublet; t, triplet; q, quartet; and m, multiplet. Spectral data (IR, mass, and NMR spectra) confirmed the structures of the synthesized compounds. The progress and success of each step, as well as the purity determinations of the obtained compounds were controlled and confirmed by thin layer chromatography (TLC) on readymade silica gel plates (Merck) using chloroform : methanol (9 : 1) as mobile phase. Spots were detected and visualized under the UV light. The X-ray diffraction (XRD) pattern related to the structural phases of the prepared catalyst was accomplished using a JEOL JEM-1010 electron microscope and JEOL JSM-6100 microscope with (Cu kα radiation, $\lambda = 1.54$ Å) in the region of $2\theta = 20°$–$80°$. The surface morphology and diameter of the catalyst nanoparticles (γ-Fe_2O_3@CPTMS–guanidine@SO_3H) was studied by scanning electron microscopy (SEM) analysis data was also recorded on an FEI Quanta 200 at a 20 kV accelerating voltage. Samples were prepared by dispensing drops of an aqueous suspension of particles on to a glass plate. This was allowed to dry at room temperature and was then coated with a thin Au film. SEM and the energy dispersive X-ray spectroscopy (EDS) analyses were performed. The elemental mapping and compositional analysis was performed by energy-dispersive X-ray spectroscopy (EDX) by a Kevex, Delta Class I, equipped with the SEM instrument. To characterize the magnetic measurement of modified and unmodified nanoparticles, a varying magnetic field from −10 000 to 10 000 on a BHV-S5 vibrating sample magnetometer (VSM) was utilized at room temperature (MDKFD, University of Kashan, Kashan, Iran). All the catalyst materials were degassed by passing nitrogen overnight at 200 °C. The transmission electron microscope (TEM) images of the nanocatalyst was performed using a FEI CM200 field emission at accelerating voltage of 200 kV. The thermal gravimetric analysis (TGA) of nano-magnetic solid acid catalyst was carried out on a Shimadzu Thermogravimetric Analyzer (TG-50) in the temperature range of 25–900 °C at a heating rate of 10 °C min^{-1} in air under N_2 atmosphere. The magnetic property of the catalyst was measured using a vibrating sample magnetometer (VSM, 7400 Lake Shore). The energy dispersive X-ray spectroscopy (EDX) was performed using TESCAN Vega model instrument. The thermogravimetry and differential thermogravimetry (TG-DTG). The Fourier-transform infrared spectroscopy (FT-IR). The field emission scanning electron microscopy (FESEM).

4.2. Synthesis of γ-Fe_2O_3 and chloro-functionalized γ-Fe_2O_3@CPTMS and γ-Fe_2O_3@CPTMS–guanidine

γ-Fe_2O_3 NPs and chloro-functionalized γ-Fe_2O_3@CPTMS were synthesized by the conventional co-precipitation procedure.[24]

4.3. Synthesis of γ-Fe_2O_3@CPTMS–guanidine@SO_3H

The suspension of γ-Fe_2O_3@CPTMS–guanidine (1 g) in methanol (20 ml) was sonicated in 100 ml round-bottom flask for 35

Table 1 Optimization of reaction conditions for compound **4a**

Entry	Catalyst (g)	Power	Time (min)	Yield[ab] (%)
1	—	180	30	Nil
2	$ClSO_3H$ (0.005)	180	15	81
3	γ-Fe_2O_3 (0.05)	180	15	45
4	Fe_2O_3@CPTMS (0.05)	180	15	50
5	γ-Fe_2O_3@SiO_2–guanidine@SO_3H (0.05)	180	15	92
6	γ-Fe_2O_3@SiO_2–guanidine@SO_3H (0.05)	300	10	89
7	γ-Fe_2O_3@SiO_2–guanidine@SO_3H (0.05)	100	25	85
8	γ-Fe_2O_3@SiO_2–guanidine@SO_3H (0.05)	180	15	92
9	γ-Fe_2O_3@SiO_2–guanidine@SO_3H (0.05)	180	10	90
10	γ-Fe_2O_3@SiO_2–guanidine@SO_3H (0.08)	180	10	92
11	γ-Fe_2O_3@SiO_2–guanidine@SO_3H (0.015)	180	20	35

[a] It was at various microwave powers (100–300 W) at range of 40–100 °C in EtOH that the reaction was tested. [b] Isolated yields.

Table 2 Preparation of quinazolin-4(3*H*)-one derivatives in the presence of γ-Fe_2O_3@CPTMS–guanidine@SO_3H (0.05 g) as catalyst under microwave irradiation (180 W, max. 70 °C) conditions in solvent-free condition

Entry	Name	RNH_2	Time (h)	Yield[a] (%)	Mp (obs) (°C)	Mp (lit) (°C)
1	**4a**	NH_4OAC	15	92	287–289 °C	230–232 °C (ref. 29)
2	**4b**	Propyl amine	20	92	81–83 °C	82–83 °C (ref. 30)
3	**4c**	Butyl amine	20	90	88–90 °C	89 °C (ref. 31)
4	**4d**	Cyclohexyl amine	20	92	289–291 °C	>300 °C (ref. 32)
5	**4e**	Benzyl amine	15	55	220–223 °C	230–231 °C (ref. 34)
6	**4f**	Aniline	15	68	145–146 °C	147–148 °C (ref. 33)
7	**4g**	4- Chloro aniline	20	70	154–155 °C	156–158 °C (ref. 33)
8	**4h**	4- Nitro aniline	20	80	193 °C	190–193 °C (ref. 33)
9	**4i**	4-Methoxy aniline	20	62	173 °C	169–171 °C (ref. 33)
10	**4j**	4-Methyl aniline	20	40	153–155 °C	149–150 °C (ref. 33)
11	—	3- Nitro aniline	20	35	170–173 °C	171–172 °C (ref. 32)
12	**4k**	4-Bromo aniline	15	90	159–161 °C	159–161 °C (ref. 35)
13	**4l**	2,5-Dimethoxy aniline	15	70	170–173 °C	171–172 °C (ref. 33)
14	**4m**	*n*-Phenylsulfonyl amine	20	50	138–139 °C	138–139 °C (ref. 35)
15	**4n**	Triflouromethoxy aniline	20	35	223.0 °C	223 °C (ref. 36)
16	**4o**	3-Aminophenol	20	65	114.5 °C	115 °C (ref. 36)
17	**4p**	2-Methyl-4-phenyl-1*H*-imidazole	15	91	257–259 °C	Present work
18	**4q**	2-(Benzo[*d*]thiazol-2-yl)phenol	15	92	280–282 °C	Present work

[a] Isolated yields.

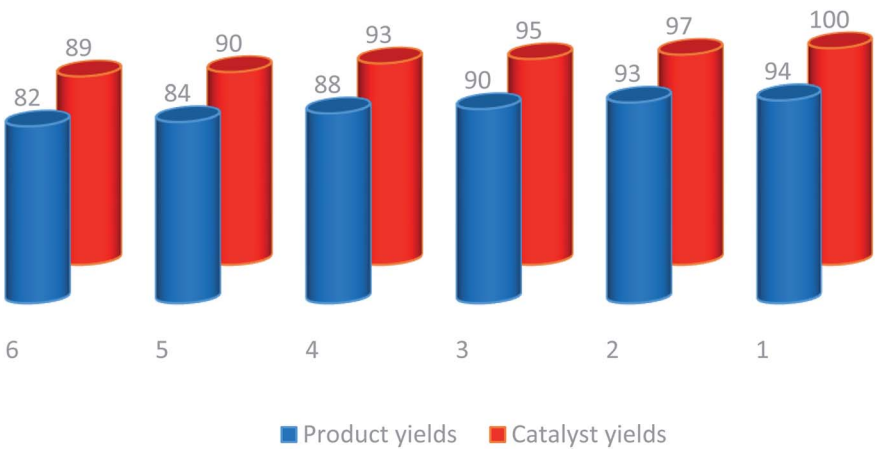

Fig. 11 Reusability of nanocatalyst.

Table 3 Comparison of the efficiency of γ-Fe_2O_3@CPTMS–guanidine@SO_3H with other reported catalysts in literature

Entry	Catalyst/condition	Time (min)	Yield[ab] (%)	Ref.
1	$TiCl_4$/Zn, THF, reflux	240 min	83	Previous work[37]
2	N_2H_4/H_2O, reflux	210 min	80	Previous work[38]
3	$KMnO_4$/AcOH, reflux	360 min	65	Previous work[39]
4	γ-Fe_2O_3@CPTMS–guanidine@SO_3H/solvent free, MW (180 W, max. 70 °C)	15 min	92	Present work

[a] Isolated yields. [b] The reaction was carried out under microwave irradiation (MW) conditions.

minutes and, then, sulfonic acid (1 ml) was added dropwise. Afterwards, it was at 30 °C that the reaction mixture was stirred overnight. Finally, we aimed at collecting the precipitates, applying an external magnet, which were washed three times with EtOH and diethyl ether and, then, dried in an oven at 50 °C for 10 h (Scheme 2).

4.4. General procedure for the synthesis of new quinazolin-4(3*H*)-one derivative

Herein, a multicomponent reaction was performed between different amines, antranilic acids and acetic anhydride in the presence of γ-Fe_2O_3@CPTMS–guanidine to synthesize 3-substituted 2-methylquinazoline- 4-(3*H*)-one derivatives

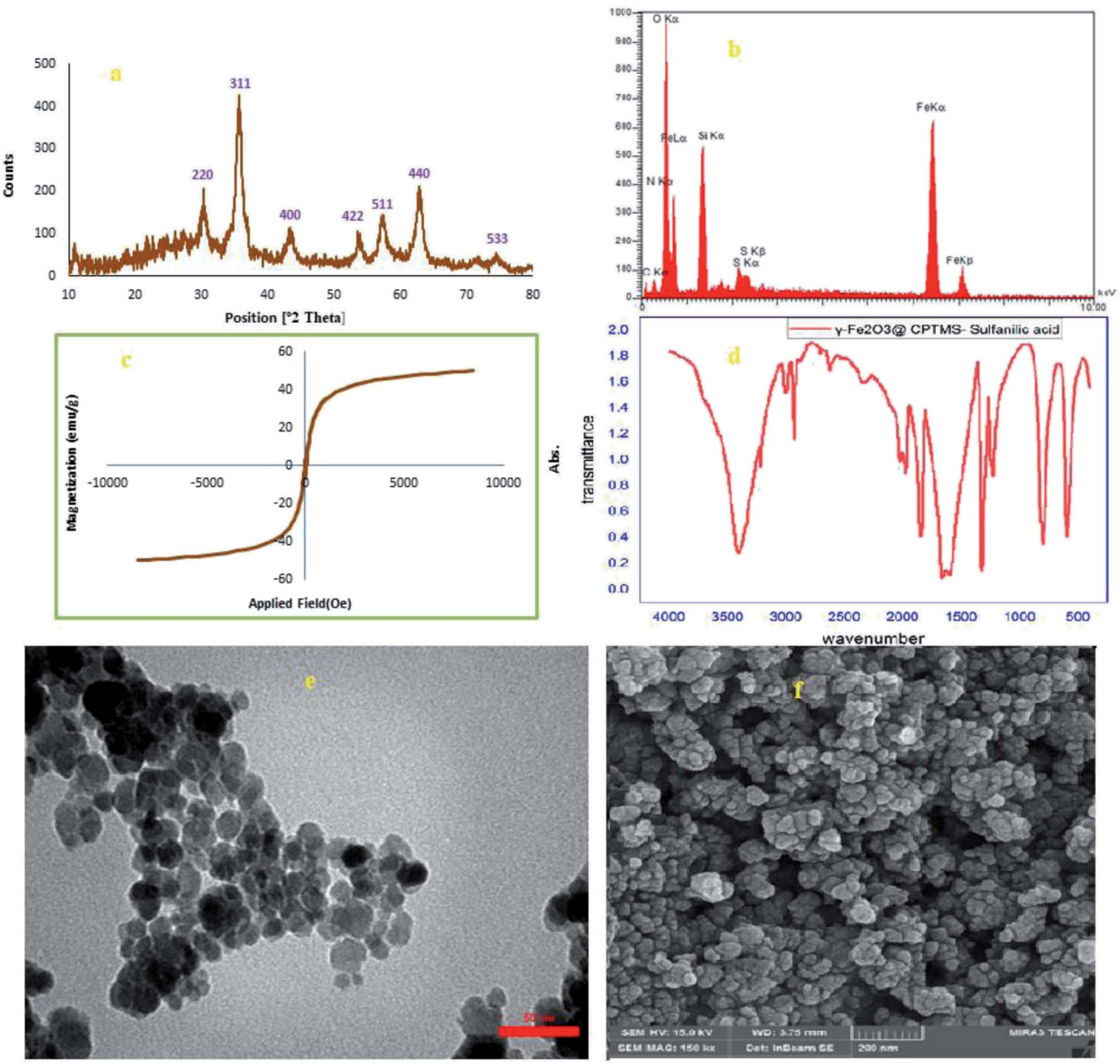

Fig. 12 (a) XRD, (b) EDAX, (c) VSM, (d) FT-IR, (e) TEM, and (f) SEM analysis of the recovered Fe_3O_4@PABA–Cu(II).

(Scheme 1). Afterwards, a mixture of acetic anhydride (1.2 mmol) with selected aromatic amines (1 mmol), anthranilic acid (1 mmol) and γ-Fe_2O_3@CPTMS–guanidine (0.05 g) was added to a canonical flask (25 ml). Subsequently, as shown in Table 2, the mixture was irradiated in a microwave at 180 W, whose maximum internal temperature was 70 °C. When the reaction was completed, as it was monitored by TLC, we aimed at separating the catalyst by an external magnet. After we filtered the precipitated solid, the pure product was obtained. Moreover, column chromatography was applied for the compounds that did not reach this level, as it was on silica gel applying petroleum ether/ethyl acetate as elution.

Conflicts of interest

There are no conflicts to declare.

Acknowledgements

The authors thankful the Tehran North Branch, Islamic Azad University and Aja University of Medical Sciences for providing laboratory facilities to carry out this research.

References

1 P. T. Anastas and J. C. Warner, Principles of green chemistry, *Green Chem. Theory Practice*, 1998, 29.

2 K. Niknam, N. Borazjani, R. Rashidian and A. Jamali, Silica-bonded N-propylpiperazine sodium *n*-propionate as recyclable catalyst for synthesis of 4H-pyran derivatives, *Chin. J. Catal.*, 2013, **34**(12), 2245–2254.

3 L. Ma'mani, M. Sheykhan, A. Heydari, M. Faraji and Y. Yamini, Sulfonic acid supported on hydroxyapatite-encapsulated-γ-Fe_2O_3 nanocrystallites as a magnetically Brønsted acid for N-formylation of amines, *Appl. Catal., A*, 2010, **377**(1–2), 64–69.

4 J. Deng, L. P. Mo, F. Y. Zhao, L. L. Hou, L. Yang and Z. H. Zhang, Sulfonic acid supported on hydroxyapatite-encapsulated-γ-Fe_2O_3 nanocrystallites as a magnetically separable catalyst for one-pot reductive amination of carbonyl compounds, *Green Chem.*, 2011, **13**(9), 2576–2584.

5 N. Koukabi, E. Kolvari, M. A. Zolfigol, A. Khazaei, B. S. Shaghasemi and B. Fasahati, A Magnetic Particle-Supported Sulfonic Acid Catalyst: Tuning Catalytic Activity between Homogeneous and Heterogeneous Catalysis, *Adv. Synth. Catal.*, 2012, **354**, 2001–2008.

6 E. Rafiee and S. Eavani, $H_3PW_{12}O_{40}$ supported on silica-encapsulated γ-Fe_2O_3 nanoparticles: a novel magnetically-recoverable catalyst for three-component Mannich-type reactions in water, *Green Chem.*, 201, **13**(8), 2116–2122.

7 S. Shylesh, V. Schünemann and W. R. Thiel, Magnetically separable nanocatalysts: bridges between homogeneous and heterogeneous catalysis, *Angew. Chem., Int. Ed.*, 2010, **49**(20), 3428–3459.

8 S. Rostamnia, K. Lamei, M. Mohammadquli, M. Sheykhan and A. Heydari, Nanomagnetically modified sulfuric acid (γ-Fe_2O_3@SiO_2-OSO_3H): an efficient, fast, and reusable green catalyst for the Ugi-like Groebke-Blackburn-Bienaymé three-component reaction under solvent-free conditions, *Tetrahedron Lett.*, 2012, **53**(39), 5257–5260.

9 A. Kong, P. Wang, H. Zhang, F. Yang, S. Huang and Y. Shan, One-pot fabrication of magnetically recoverable acid nanocatalyst, heteropolyacids/chitosan/Fe_3O_4, and its catalytic performance, *Appl. Catal., A*, 2012, **417**, 183–189.

10 M. Okamura, A. Takagaki, M. Toda, J. N. Kondo, K. Domen, T. Tatsumi and S. Hayashi, Acid-catalyzed reactions on flexible polycyclic aromatic carbon in amorphous carbon, *Chem. Mater.*, 2006, **18**(13), 3039–3045.

11 J. B. Bariwal, J. C. Trivedi and E. V. van der Eycken, Microwave irradiation and multicomponent reactions, in *Synthesis of Heterocycles viaMulticomponent Reactions II*, Springer, Berlin, Heidelberg, 2010, vol. 25, pp. 169–230.

12 D. Garella, E. Borretto, A. Di Stilo, K. Martina and G. Cravotto, Microwave-assisted synthesis of N-heterocycles in medicinal chemistry, *MedChemComm*, 2013, **4**(10), 1323–1343.

13 J. Tang, L. Wang, Y. Yao, L. Zhang and W. Wang, One-pot synthesis of 2-amino-3-cyanopyridine derivatives catalyzed by ytterbium perfluorooctanoate [$Yb(PFO)_3$], *Tetrahedron Lett.*, 2011, **52**(4), 509–511.

14 L. V. Frolova, I. Malik, P. Y. Uglinskii, S. Rogelj, A. Kornienko and I. V. Magedov, Multicomponent synthesis of 2,3-dihydrochromeno [4,3-*d*] pyrazolo [3,4-*b*] pyridine-1,6-diones: a novel heterocyclic scaffold with antibacterial activity, *Tetrahedron Lett.*, 2011, **52**(49), 6643–6645.

15 D. He, M. Wang, S. Zhao, Y. Shu, H. Zeng, C. Xiao and Y. Liu, Pharmaceutical prospects of naturally occurring quinazolinone and its derivatives, *Fitoterapia*, 2017, **119**, 136–149.

16 J. B. Koepfli, J. F. Mead and J. A. Brockman Jr, An alkaloid with high antimalarial activity from Dichroa Febrifuga1, *J. Am. Chem. Soc.*, 1947, **69**(7), 1837.

17 G. Honda and M. Tabata, Isolation of antifungal principle tryptanthrin, from Strobilanthes cusia O. Kuntze, *Planta Med.*, 1979, **36**(05), 85–86.

18 Y. Rao, H. Liu, L. Gao, H. Yu, J. H. Tan, T. M. Ou and Z. S. Huang, Discovery of natural alkaloid bouchardatine as a novel inhibitor of adipogenesis/lipogenesis in 3T3-L1 adipocytes, *Bioorg. Med. Chem.*, 2015, **23**(15), 4719–4727.

19 G. Huang, A. Drakopoulos, M. Saedtler, H. Zou, L. Meinel, J. Heilmann and M. Decker, Cytotoxic properties of the alkaloid rutaecarpine and its oligocyclic derivatives and chemical modifications to enhance water-solubility, *Bioorg. Med. Chem. Lett.*, 2017, **27**(21), 4937–4941.

20 V. Duraipandiyan, N. A. Al-Dhabi, C. Balachandran, S. Ignacimuthu, C. Sankar and K. Balakrishna, Antimicrobial, antioxidant, and cytotoxic properties of vasicine acetate synthesized from vasicine isolated from Adhatoda vasica L, *BioMed Res. Int.*, 2015, **2015**, 727304–727310.

21 H. C. Ko, Y. H. Wang, K. T. Liou, C. M. Chen, C. H. Chen, W. Y. Wang and Y. C. Shen, Anti-inflammatory effects and mechanisms of the ethanol extract of Evodia rutaecarpa

and its bioactive components on neutrophils and microglial cells, *Eur. J. Pharmacol.*, 2007, **555**(2–3), 211–217.

22 M. M. Sadek, Antifeedant and toxic activity of Adhatoda vasica leaf extract against Spodoptera littoralis (Lep., Noctuidae), *J. Appl. Entomol.*, 2003, **127**(7), 396–404.

23 A. Astulla, K. Zaima, Y. Matsuno, Y. Hirasawa, W. Ekasari, A. Widyawaruyanti and H. Morita, Alkaloids from the seeds of Peganum harmala showing antiplasmodial and vasorelaxant activities, *J. Nat. Med.*, 2008, **62**(4), 470–472.

24 M. Akhavan, N. Foroughifar, H. Pasdar and A. Khajeh-Amiri, Bekhradnia, Copper (II)-complex functionalized magnetite nanoparticles: a highly efficient heterogeneous nanocatalyst for the synthesis of 5-arylidenthiazolidine-2, 4-diones and 5-arylidene-2-thioxothiazolidin-4-one, *Transition Met. Chem.*, 2017, **42**(6), 543–552.

25 M. Demeunynck and I. Baussanne, Survey of recent literature related to the biologically active 4 (3*H*)-quinazolinones containing fused heterocycles, *Curr. Med. Chem.*, 2013, **20**(6), 794–814.

26 C. U. Maheswari, G. S. Kumar, M. Venkateshwar, R. A. Kumar, M. L. Kantam and K. R. Reddy, Highly efficient one-pot synthesis of 2-substituted quinazolines and 4H-benzo [d][1, 3] oxazines via cross dehydrogenative coupling using sodium hypochlorite, *Adv. Synth. Catal.*, 2010, **352**(2–3), 341–346.

27 N. Coşkun and M. Çetin, Synthesis of 2-aryl-1, 2, 3, 4-tetrahydroquinazolin-1-ols and their conversion to 7-aryl-9H-6-oxa-5, 8-diaza-benzocycloheptenes, *Tetrahedron Lett.*, 2004, **45**(49), 8973–8975.

28 Z. Esam, M. Akhavan, A. Bekhradnia, M. Mohammadi and S. Tourani, A Novel Magnetic Immobilized Para-Aminobenzoic Acid-Cu (II) Complex: A Green, Efficient and Reusable Catalyst for Aldol Condensation Reactions in Green Media, *Catal. Lett.*, 2020, **150**, 3112–3131.

29 M. Akhavan, N. Foroughifar, H. Pasdar and A. Bekhradnia, Green Synthesis, Biological Activity Evaluation, and Molecular Docking Studies of Aryl Alkylidene 2, 4-thiazolidinedione and Rhodanine Derivatives as Antimicrobial Agents, *Comb. Chem. High Throughput Screening*, 2019, **22**(10), 716–727.

30 M. Akhavan and A. Bekhradnia, Stereoselective synthesis of spirocyclic pyrrolidines/pyrrolizidines/pyrrolothiazolidines using l-proline functionalized manganese ferrite nanorods as a novel heterogeneous catalyst, *RSC Adv.*, 2021, **11**(24), 14755–14768.

31 Z. Esam, M. Akhavan and A. Bekhradnia, One-pot multicomponent synthesis of novel 2-(piperazin-1-yl) quinoxaline and benzimidazole derivatives, using a novel sulfamic acid functionalized Fe3O4 MNPs as highly effective nanocatalyst, *Appl. Organomet. Chem.*, 2021, **35**(1), e6005.

32 M. Akhavan, N. Foroughifar, H. Pasdar and A. Bekhradnia, Green Chemical Synthesis and Biological Evaluation of Novel N-substituted Rhodanine Derivatives as Potential Antifungal Agents, *J. Mazandaran Univ. Med. Sci.*, 2020, **29**(182), 82–90.

33 V. S. Kudale and J. J. Wang, Metal-free C–H methylation and acetylation of heteroarenes with PEG-400, *Green Chem.*, 2020, **22**(11), 3506–3511.

34 H. Nakano, N. Kutsumura and T. Saito, Functionalized Carbodiimide Mediated Synthesis of 2, 3-Disubstituted Quinazolin-4 (3H)-ones via the Tandem Strategy of C-Nucleophilic Addition and Intramolecular NH-Substitution Cyclization, *Synthesis*, 2012, **44**(20), 3179–3184.

35 S. Malhotra, S. K. Koul, S. Singh, G. B. Singh and K. L. Dhar, Studies on Some Biologically Active Azepinoquinazolines. Part 2. An Approach to Effective Antiinflammatory Drug, *Chem. Inf.*, 1989, **20**(30).

36 O. O. Ajani, Expeditious synthesis and spectroscopic characterization of 2-methyl-3-substituted-quinazolin-4 (3H)-one derivatives, *Orient. J. Chem.*, 2017, **33**(2), 562–574.

37 W. Xu, X. R. Zhu, P. C. Qian, X. G. Zhang and C. L. Deng, Copper-catalyzed tandem reaction of 2-aminobenzamides with tertiary amines for the synthesis of quinazolinone derivatives, *Synlett*, 2016, **27**(20), 2851–2857.

38 S. Xue, J. McKenna, W. C. Shieh and O. Repic, A facile synthesis of C 2, N 3-disubstituted-4-quinazolone, *J. Org. Chem.*, 2004, **69**(19), 6474–6477.

39 A. Khalafi-Nezhad, S. M. Haghighi, A. Purkhosrow and F. Panahi, An efficient one-pot access to quinazolinone derivatives using TiO_2 nanoparticles as catalyst: synthesis and vasorelaxant activity evaluation, *Synlett*, 2012, **23**(06), 920–924.